

**Tie Hu**  
**Peter K. Allen**

Department of Computer Science,  
Columbia University,  
New York, NY 10027,  
USA  
allen@cs.columbia.edu

**Nancy J. Hogle**  
**Dennis L. Fowler**

Department of Surgery,  
Columbia University,  
New York, NY 10032,  
USA

# Insertable Surgical Imaging Device with Pan, Tilt, Zoom, and Lighting

## Abstract

*In this paper we describe work we have done in developing an insertable surgical imaging device with multiple degrees of freedom for minimally invasive surgery. The device is fully insertable into the abdomen using standard 12 mm trocars. It consists of a modular camera and lens system which has pan and tilt capability provided by two small DC servo motors. It also has its own integrated lighting system that is part of the camera assembly. Once the camera is inserted into the abdomen, the insertion port is available for additional tooling, motivating the idea of single-port surgery. A third zoom axis has been designed for the camera as well, allowing close-up and far-away imaging of surgical sites with a single camera unit. In animal tests with the device we have performed surgical procedures including cholecystectomy, appendectomy, running (measuring) the bowel, suturing, and nephrectomy. Preliminary tests suggest that the new device may have advantages over a standard laparoscope including the following.*

- *Low-cost and simple design.*
- *Easier and more intuitive to use than a standard laparoscope.*
- *Joystick operation requires no specialized operator training.*
- *Pan/tilt functions provide a large imaging volume not restricted by the fulcrum point of standard laparoscope.*

- *Time to perform procedures was better than or equivalent to a standard laparoscope.*

*We believe these insertable platforms will be an integral part of future surgical systems. The platforms can be used with tooling as well as imaging devices, allowing many surgical procedures to be performed using such a system.*

**KEY WORDS**—endoscope, minimally invasive surgery, surgical robot, laparoscopy.

## 1. Introduction

Our goal is to enhance and improve surgical procedures by placing small, mobile, multi-function platforms inside the body that can begin to assume some of the tasks associated with surgery (Oleynikov et al. 2005). We want to create a feedback loop between new, insertable sensor technology and effectors we are developing, with both surgeons and computers in the information-processing/control loop. We envision surgery in the future as radically different from today. This is clearly a trend that has been well established as minimal-access surgical procedures continue to expand. Accompanying this expansion has been new thrusts in computer and robotic technologies that make automated surgery, if not feasible, an approachable goal. It is not difficult to foresee teams of insertable robots performing surgical tasks inside the body under control of both the surgeon and computer. The benefits of such an approach are well documented: greater precision, less trauma to the patient, and improved outcomes (Peters and Bartels 1993; Vierra 1995; Schwenk et al. 1999). One factor limiting this expansion is that the laparoscopic paradigm of pushing

long sticks into small openings is still the state-of-the-art, even among surgical robots such as the da Vinci system by Intuitive Surgical (Guthart and Salisbury 2000). While this paradigm has been enormously successful, and has spurred development of new methods and devices, it is ultimately limiting in what it can achieve. Our intent is to go beyond this paradigm, and remotely place sensors and effectors into the body cavity where they can perform surgical and imaging tasks unfettered by traditional endoscopic instrument design.

The basic architecture of the endoscope has not been fundamentally changed since the invention of the rod-lens by Hopkins and cold light source of fiberoptics by Karl Storz in the 1950s (Fuchs 2006). Traditional endoscopes use fiberoptics to deliver the light into the abdomen and the rod-lens to transmit the image back to the CCD camera sensor. This approach has a number of limitations, such as narrow imaging, limited work space, counter intuitive motion, and additional incisions for the endoscope. Since the surgeon is generally working with both hands holding other instruments, an assistant is necessary to hold the endoscope steady and move it as required. Recent work in robotics has sought to automate that task. One example is the AESOP medical robot that can orient a traditional endoscope using a robotic arm that is controlled by spoken commands (Geis et al. 1996). A similar principle is used in the da Vinci surgical robots (Guthart and Salisbury 2000). A simpler robotic endoscope manipulator that can be placed directly over the insertion point was developed at INRIA (Berkelman et al. 2002; Ma and Berkelman 2007). However, none of these systems addresses the fundamentally limited range of motion of the endoscope. The fulcrum point created by the abdominal wall restricts the motion of the scope to four degrees of freedom (DOFs), so that the only translation possible is along the camera axis.

There is some related research on new designs for endoscopes. One system uses a traditional rigid rod endoscope but adds a motor that rotates a 90° mirror at the end of the scope to provide an additional DOF (Gao et al. 1998). Another system is essentially a multi-link arm that positions a camera using piezoelectric actuators (Ikuta et al. 1994). Theoretically this robot would provide many different viewing angles for an attached camera, but the authors provide no information about the safety of using piezoelectric electric elements, and do not appear to have attempted any tests within living animals or humans. The pill camera (Yu 2002) is an example of a camera that operates entirely within the body. It is able to image sections of the small intestine that an endoscope cannot reach. However, it does not have any means of actuation and simply relies on peristalsis for locomotion. A self-propelling endoscope with a miniature robot arm could move through the colon by inchworm locomotion (Peirs et al. 2001). Magnetic anchoring was used to maneuver the locomotion of a micro camera in the body (Park et al. 2007). Since there are no additional actuators in the camera, the view point is limited by the camera orientation. Other examples of new ideas in designing

surgical robots include Dachs and Peine (2006) who developed a six-DOF surgical robot (Laprotek from EndoVia, Inc) which eliminates the dependence on pivoting about the incision point. Sastry et al. (1997) presented the idea of milli-robots for remote, minimally invasive surgery that can increase the dexterity and the reachable workspace of the surgeon.

We have been focusing on developing an inexpensive, compact, insertable endoscopic camera with multiple DOFs. In this paper, we describe our insertable pan/tilt endoscope with integrated light source that we have built and tested in five *in vivo* animal tests which included appendectomy, cholecystectomy, running(measuring) the bowel, suturing, and nephrectomy. The initial results suggest that the device is easier to use and control than a standard laparoscope. Our imaging device only requires a single access port and has more flexibility, as it is inside the body cavity and can obtain images from a number of controllable directions. There is no need for extensive training with this device as with a standard laparoscopic since it is operated by a simple joystick. Standard laparoscopes have counterintuitive motions owing to the pivoting about the insertion point (e.g. to move the laparoscope to the right, the external part of the unit is moved to the left, pivoting on the insertion point). This can cause confusion for untrained operators. Our device can image a large view volume and is not restricted by the fulcrum insertion point of a standard laparoscope, allowing the surgeon greater flexibility in seeing the inside of the abdominal cavity. Our tests have also shown that zooming capabilities are desirable for such a device, and we also present a design for a zooming capability that will add an extra DOF to our device, extending its utility during surgery.

## 2. Materials and Methods

### 2.1. Prototype I

In earlier work (Miller et al. 2004) we designed a robotically actuated, multi-camera five-DOF system that can be inserted entirely within the abdominal cavity. Once inserted, the device is rigidly fixed to the interior abdominal wall to provide a stable base for the actuated cameras. After situating the device near the operation site, the cameras can be extracted, and look upon the area of interest. In Figure 1, the top image shows simulated device with cameras retracted for body cavity insertion, and the bottom image shows the device with cameras extended for imaging. The design of the device allows it to be fully inserted into the body cavity through a traditional laparoscopic incision.

To test this design, we have built a single camera prototype with three DOFs (pan, tilt, translation). Figure 2 shows the different DOFs. Figure 3 shows the initial tracking system we have developed to have the camera follow a target automatically. Real-time autonomous tracking of moving objects such as organs, surgical instruments or anatomical tissue can

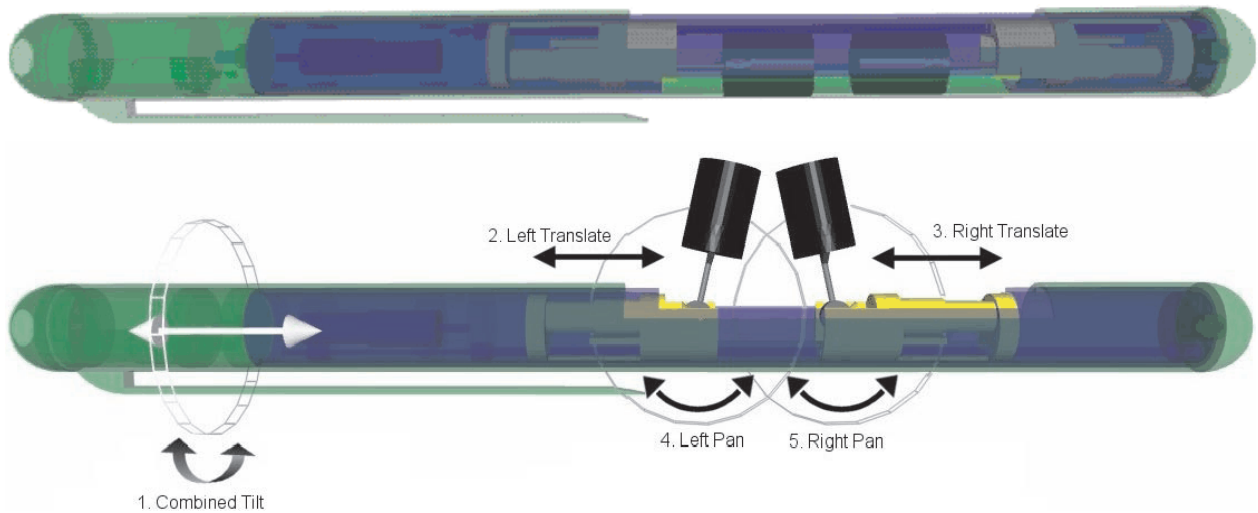


Fig. 1. Design of Prototype I: five-DOF insertable camera device. Top: device with cameras retracted. Bottom: device with cameras extracted.

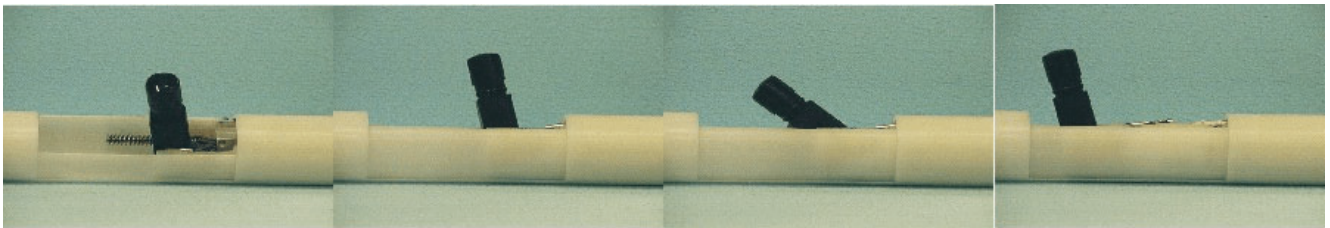


Fig. 2. Prototype I *in-vivo* imaging device. This prototype has a single camera, but the platform is designed to have two cameras. This sequence demonstrates the motions that can be achieved for a single camera. First tilting about the central device axis is shown, then panning about an orthogonal axis, and finally translation. The second camera will have a common tilt axis and independent pan and translation axes.

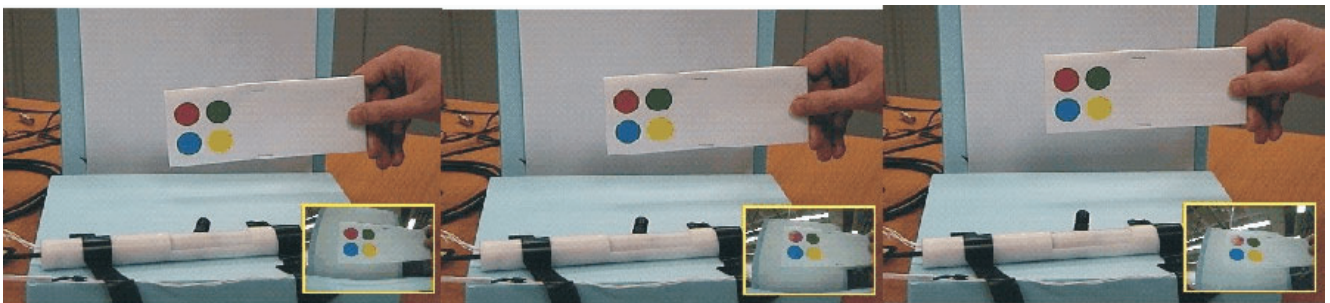


Fig. 3. Early visual servoing experiments with Prototype I demonstrate that the system can keep a moving target pattern within its field of view. Image-based visual servoing is used to track the target automatically.

be done with the device. Image processing is used to identify a target region of the scene based upon its RGB color components. These components can be seeded by the operator who

can window a region to be tracked. The motor control system is open loop, so the vision system can be used to servo the position error of the cameras. Proportional control can be used



Fig. 4. Prototype I was used in a suturing experiment within a laparoscopic training box. The image provided by the device was sufficiently clear to perform the task without using any additional image sources. The surgeon's assistant was able to adjust the view at the surgeon's request by joystick control of the camera's pan, tilt and translation axes.



Fig. 5. Prototype I was used in another task that required motions over greater distances and was performed within the training box. Again the assistant was able to keep the activity within the field of view of the camera. This sequence more clearly shows the motions of the camera.

to keep a tracked region in the center of the image. Once the region is identified, the pixel coordinates of its centroid can be calculated. Then, using a scaling gain, the imaging device's pan and tilt axes can be moved to keep the target centered in the image. Each axis (pan and tilt) is controlled independently. The vertical (horizontal) error measured in image pixels from the image center is used to control the tilt (pan) axis, where the velocity is proportional to the vertical (horizontal) pixel error. The control signals are updated 30 times per second.

Figure 4 shows an initial experiment in a laparoscopic training box. The device was mounted inside the box, and a surgeon was able to perform a simulated suturing task using the image from the prototype device. The camera was manually controlled by an assistant using a joystick responding to the surgeon's instructions. Figure 5 shows the device being moved to explore the entire viewing field, allowing the surgeon to see a greater view volume than a traditional laparoscopes. A video of the device is available as a multimedia extension (see appendix).

The outer shell of Prototype I (see Figure 2) device is a tube that is 22 mm in diameter, 19 cm long, and the cabling emerges from the proximal end. The first motor, which controls the tilt-

ing motion of the cameras, is parallel with the central axis of the shell and is near the proximal end. This motor rotates an inner shell that contains both cameras and the other motors. A 5.8 cm long section of the outer tube is cut away at the distal end to allow the cameras to tilt 180° when they are extracted.

This device was tested by six surgeons in a mock up using a surgical training box (Strong et al. 2005). The surgeons each completed a series of five validated tests (MISTELS: McGill Inanimate System for the Training and Evaluation of Laparoscopic Skill). Each surgeon completed the series of tests using the prototype imaging platform once and a standard video laparoscopy system once. The performance of each surgeon using the new imaging platform was compared with their performance using the laparoscope. There was no significant difference in the performance on the tests for any surgeon using the two imaging systems.

## 2.2. Prototype II

We have designed a second-generation device that improves upon the design of our initial device described above (Hu et al.

2007, 2008a). Our design goals for the new prototype included reducing the device size and the inclusion of an integrated light source. This necessitated some design tradeoffs while striving to keep the functionality of Prototype I. The device diameter was primarily a function of the motor diameters, and by removing motors and hence DOFs, we were able to reduce the device's size. Clinical experience dictated that the translational DOF was the least important for imaging, and removing the translation capability for each camera reduced the motor count by two. We then decided to build a single camera module, which reduced the motor count by an additional motor. This left a two-motor design with pan and tilt axes for a single camera module. We also replaced the camera used in Prototype I, which was 8 mm in diameter, with a smaller 6.5 mm diameter device (see Section 2.2.3). The total length of the device is 110 mm, and the diameter is 11 mm, and it can be inserted into a standard 12 mm trocar.

We also needed to include a light source with the device. Standard fiberoptic sources would require high power and large bending moments, so we designed an LED array that fit around the camera module, and provided lighting with low power requirements as well.

Although Prototype II has only a single camera, we have subsequently built a stereo camera device that uses a similar design as Prototype II by mounting two cameras side by side in a single camera module, thus sharing the pan/tilt axes but providing stereo three-dimensional imaging. Including two cameras in a side-by-side design increases the device's diameter to 15 mm. Details of this device are beyond the scope of this paper, but may be found in (Hu et al. 2008b).

We make use of modular design to make the device components interchangeable and extendable. The current system includes a user-friendly interface, making it easier to control the camera's DOF using natural motions. It consists of a pan/tilt motorized CCD camera with illumination components, control interface driver, PC, and joystick controller. After the surgeon anchors the camera onto the abdomen wall, they can use the joystick to position the camera to the desired surgical viewpoint using the pan and tilt motions. The intensity of illumination can be adjusted manually through the control panel. Figure 6 shows the CAD model of the device. Figure 7 shows images of the implemented prototype device, with integrated lighting and pan/tilt axes.

### 2.2.1. Design of the Control System

Figure 8 shows the configuration of the open-loop control system. The solid-line blocks show the current system's functions, which include joystick control, video display, pan/tilt motion control, and LED light source control. The dot-line blocks show the extendable functions in the future. The future system will include a three-dimensional display, voice control, and surgical tools. The computer is a standard PC (Intel Pentium

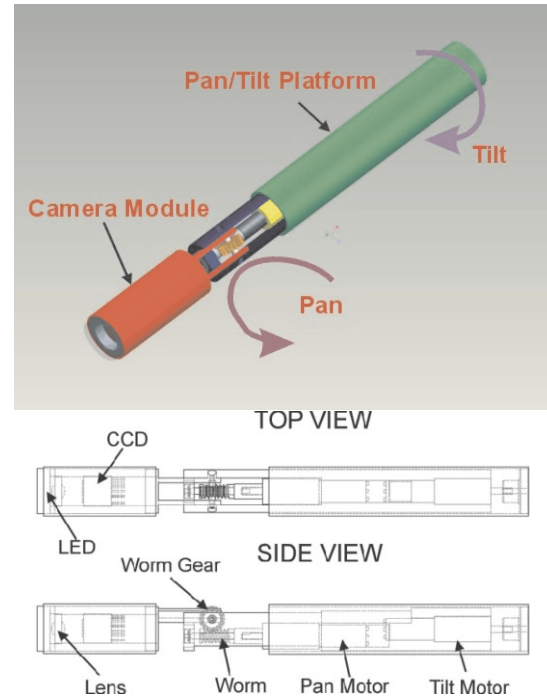


Fig. 6. CAD model of implemented Prototype II device with LED lighting and pan/tilt axes.

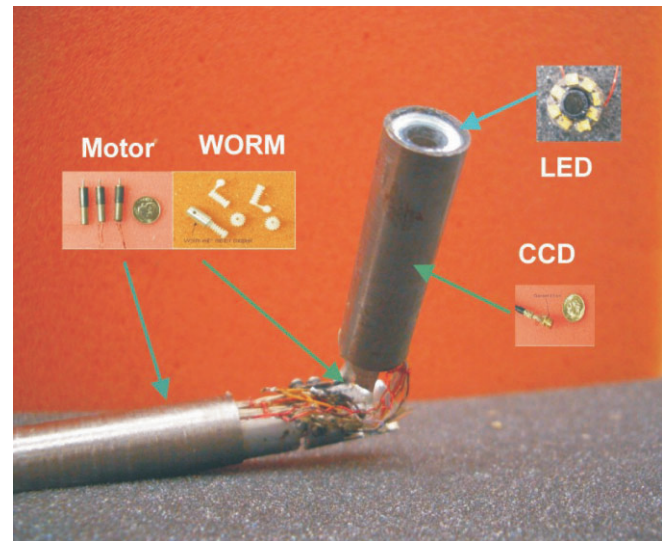


Fig. 7. Implemented Prototype II device with LED lighting and pan/tilt axes.

III, 863 MHz, 384 MB RAM) with a Hauppauge frame grabber and a motion control board. The camera system is a single-board CCD videocamera (KS600, NET USA, Inc.). This system also can digitally control the light intensity of the LED

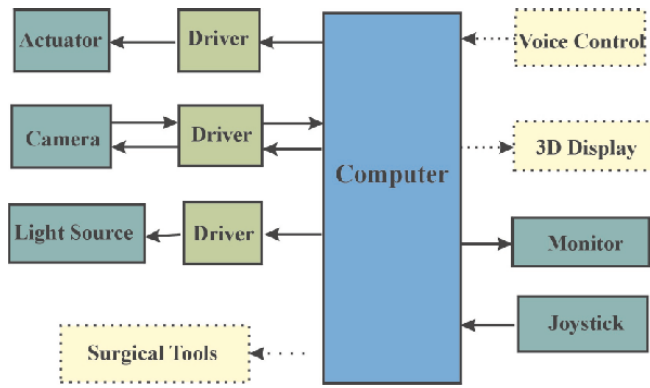


Fig. 8. Prototype II overall system configuration.

light source. The entire system consists of the PC and a 2 m long wire bundle containing control and imaging cables that connects directly to the device and which is sealed with a silicon rubber tube to protect it from body fluids.

The motion control board is a National Instruments NIDAQ PCI-6713 board with a SCB 68 break-out board, which can control the motor's direction, position and velocity. The pan and tilt motors use brushless DC motors. The NIDAQ board generates a series of control square waves to motor drivers (BLCPS.0002.8, Smoovy, Inc.), which directly output appropriate sequence current to the motor coils to drive the motor at certain speeds (the details are given in Section 2.2.4). By changing the frequency and pulses of a control square wave, we can precisely control the velocity and position of the motors. Software was developed to poll out the aileron and elevator position of the control joystick, and use these parameters to control the pan and tilt motor's velocity.

The maximum motor speed is 15,000 rpm. For the tilt motor, a 625:1 gear ratio head was used to reduce the speed and increase the motor's torque. For the pan motor, a 125:1 gear ratio head was installed and connected with a 16:1 ratio's worm gear mechanism. Therefore, the speed range for the tilt motor is from 0 to 24 rpm. The pan motion can achieve a maximum speed of  $0.79 \text{ rad s}^{-1}$ .

### 2.2.2. Design of Light Source

Most endoscopes use a Xenon light source and fiberoptics to illuminate the internal body. This method consumes power and is costly. In addition, fiberoptics are not suitable for our device because of their fragility when subjected to large bending/rotation moments. LEDs have been used as light sources for medical devices in the past, and they have the advantage of lower power, higher efficiency, lower cost, smaller package size, and longer lifespan. We selected Luxeon Portable PWT white LED (LXCL\_PWT1) as the illumination unit of the device. It has a small package size of  $2.0 \times 1.6 \times 0.7 \text{ mm}^3$ , which

can generate 26 lumens of light at 350 mA, has a color temperature of 6,500 K, and a lifespan of about 2,000 hours. For the illumination unit we designed a custom made printed circuit board (PCB) with eight LEDs. It has a size of 9 mm in external diameter, 5 mm in internal diameter, and 3 mm in thickness. The eight LEDs are serially connected and soldered in a circular PCB. It can deliver a total of 208 lumens of light, with a power consumption of 8.4 W, which is much less than a Xenon light source's 170 W power consumption. The image on the left of Figure 9 shows the CAD layout of the LED ring. A PCB plate was printed with an array of LED ring. A circular plate with one ring was cut and machined into a 9 mm circular plate. Then it was drilled with a 5 mm hole in the center. The image on the right of Figure 9 shows the finished LED board which can be soldered with the LEDs. The internal hole of the board works also as an aperture for the camera. The LED ring is inserted into the camera module and fixed in front of lens. An aluminum tube is used as the external shell of the camera module to quickly dissipate the heat generated by the LEDs. In *in-vivo* animal experiments, the light source temperature ranged from 43 to 48°C, comparable with a standard laparoscopic fiberoptic source.

### 2.2.3. Lens and Camera Design

A standard endoscope uses a series of relay lenses to transmit the image to the CCD camera sensor outside of the body. This approach protects the fragile electronics from the body fluid and moisture. However, the complicated optics and mechanical structure increases the cost of a standard endoscope and makes it almost impossible to be a disposable device. The advantage of our approach is that the standard CCD camera and lens can be used in our device, which can reduce the direct cost of the device, making the unit low cost and potentially disposable. One scenario is to dispose of low-cost components, such as the lens and mechanical components while saving the expensive parts such as CCD camera head and motors following surgical procedures. In our device, sealing has two functions, one for the protection, and the other to recycle the expensive components for future use.

We determined the optical characteristics of our lens by starting with data from a standard laparoscope which has a view angle of  $\sim 50^\circ \text{ circ}$ . For Prototype II we used a  $\frac{1}{4}$ " color video CCD camera head (Figure 10, right) with an outside diameter of 6.5 mm (NET USA Inc, CSH-1.4-V4-END-R1) in this package. The camera has active pixels of 752(H)  $\times$  582(V) at PAL system, which can provide 450 TV lines in horizontal resolution and 420 TV lines in vertical resolution. The CCD sensor has an active area of circle 4.5 mm in diameter.

Using these design specifications, we first find the appropriate focal length  $f$ :

$$f = \frac{2.25}{\tan(25 \text{ deg})} = 4.825 \text{ mm}. \quad (1)$$

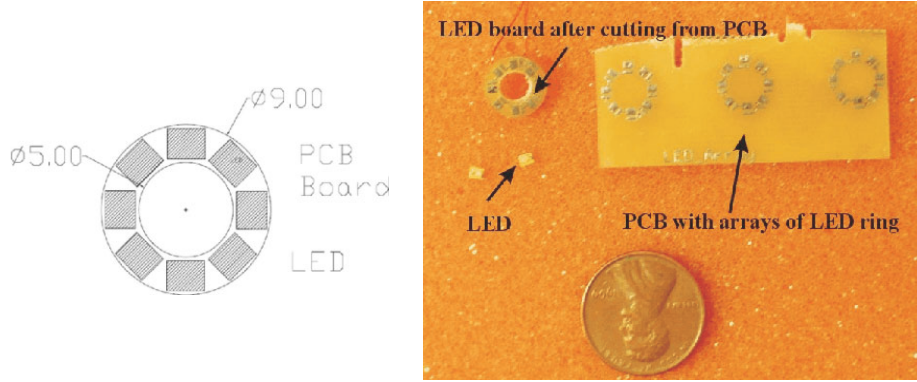


Fig. 9. Left: CAD layout of LEDs for Prototype II. Right: LED board and LED.

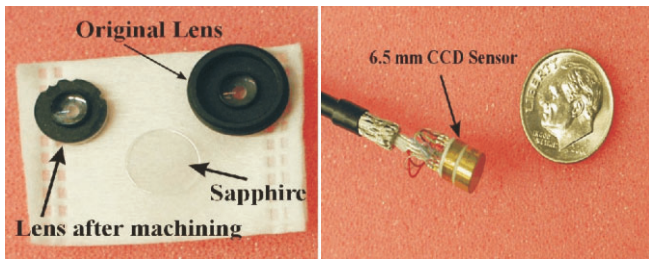


Fig. 10. Prototype II. Left: lens and sapphire. Right: CCD camera head.

The  $f$  number of the lens  $N$  is defined as  $N = \frac{f}{D}$  (Smith 2004). We chose an  $f$  number of four for our lens to allow low-light imaging. We can then calculate the lens' diameter as

$$D = \frac{f}{N} = \frac{4.825}{4} = 1.206 \text{ mm.} \quad (2)$$

We use a miniature pin-hole lens (PTS 5.0 from Universe Kogaku America) with similar optical parameters to those computed above (Figure 10, left). The external case of the lens was machined to 9 mm.

The external shell of the camera module is a stainless steel tube with external diameter of 10 mm and wall thickness of 0.25 mm. The CCD camera head is packed in a PEEK (an FDA approved plastic) tube with external diameter of 9 mm and internal diameter of 6.5 mm. Two semicircular parts tightly clamp the end of the CCD camera head wire. This design packages the fragile soldering point of the camera and insulates the terminator of the head from the stainless steel tube. A PEEK tube is fixed between the pin-hole lens and the CCD camera head. The length of the tube is exactly same as the focal length of the lens. Therefore, the image can be perfectly projected onto the CCD image sensor. The LED light source is put in front of the lens. Finally, a sapphire (Edmund Optics 9.5 mm) is put in front of the LED for protection and sealing with epoxy glue.

#### 2.2.4. Pan/Tilt Mechanism

The pan/tilt actuators are smoovy motors from Faulhaber-Group that are fixed in the internal part of device by set screws (Figure 6). A brushless DC motor (0513G, Smoovy, Inc) with 625:1 planetary gearhead (Series 06A, Smoovy, Inc.) has a length in 27.0 mm and a diameter of 5.8 mm. It can deliver a torque of 25.0 mNm at continuous operation and 37.5 mNm at intermittent operation. For a motor with 125:1 planetary gearhead, it can generate 6.0 mNm at continuous operation and 9.0 mNm at intermittent operation. We used a worm gear mechanism to pan the camera module. It can transverse the motion in a compact size and increase the output torque. The worm gear (KLEISS Gear, Inc.) has a gear reduction ratio of 16:1. A coupler was machined to connect the pan motor (125:1 gear ratio) axis and the worm (Figure 11, right). The other end of the worm is supported by a sleeve sintered brass bearing so that the motor axis could be kept aligned with the worm axis. A gear transversely rotates through the movement of the worm. The camera module is linked with the axis of the gear by a joint. Therefore, it can pan as the pan motor rotates. The axis of the tilt motor (625:1 gear ratio) is coaxially aligned with the external stainless steel tube and fixed with a coupler which is firmly attached to the external tube. A sleeve bearing made of sintered brass was machined to provide another support between the tilt part and external tube. The bearing can also reduce the friction force and smooth the tilt motion. Once the external tube is fixed on the wall of abdomen, the camera module can tilt as tilt motor rotates. The motor wires come out from the side of the tilt motor coupler. The terminators of the motors were remade to fit into a 11 mm package. The left image in Figure 11 shows the modified motor terminal. Three magnetic wires were soldered into the three terminators of the motor and epoxy glued to seal the soldering point. The pan motion ranges from 0 to 130° and the tilt motion ranges from 0 to 90°.

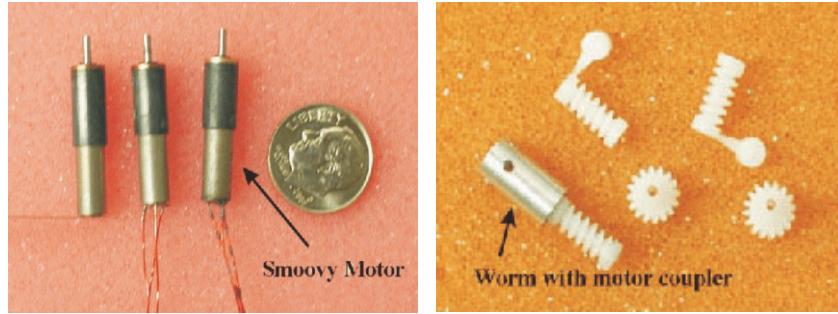


Fig. 11. Left: Smoovy motor with magnetic wire. Right: Worm gear.

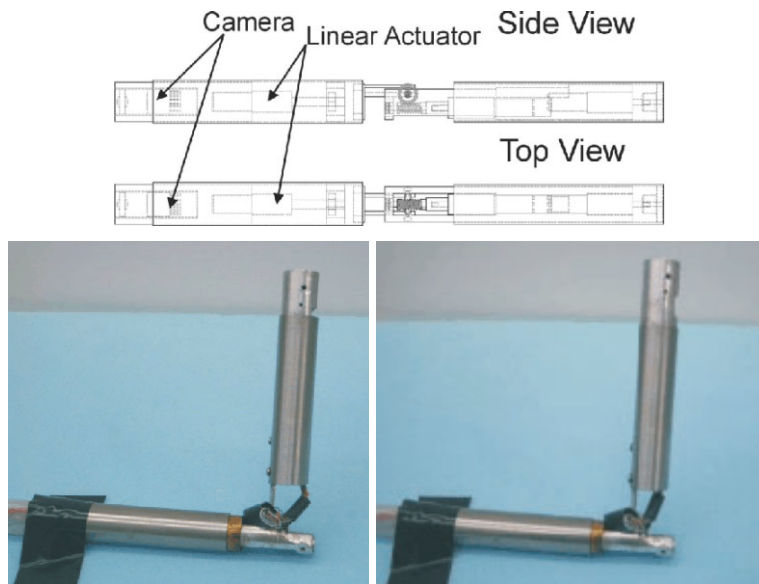


Fig. 12. Top: Prototype II CAD model of the zoom actuator system. Bottom: Prototype II camera with zoom axis. LED lighting was not included in this version of Prototype II.

**2.3. Zoom Mechanism**

From the evaluation tests, we found mechanical zoom would be a desirable function for operation. Traditional zoom lens works by moving a series of lens to change the effective focal length. It is difficult to design this type of zoom lens in such a small package. An alternative solution is to move the whole camera module back and forth to achieve the zoom function. This is the method used with standard laparoscopes.

We have designed and built a prototype device with an additional zoom DOF. The length of the device is 146 mm and the diameter is 12 mm. The top of Figure 12 shows the CAD model of new device. This design used the same pan/tilt platform as the Prototype II device, but without the LED lighting. The camera module can be driven back and forward by a linear actuator (0513-06AS2 125:1, Smoovy, Inc). This ac-

tuator is made of a 5 mm smoovy motor and precise lead screw (M2.5 × 2.5). The maximum travel speed can go up to 30 mm min<sup>-1</sup>. The travel distance is 14 mm. The external tube has an external diameter of 12 mm and an internal diameter of 11 mm. The external surface of the camera module was precisely machined to fit into the tube. The bottom of Figure 12 shows the prototyped device with zoom out and in. The pan/tilt/zoom version of Prototype II was tested for functionality without the LED lighting owing to time constraints as the LEDs required additional wiring and assembly. An external light source was used to provide illumination in these tests.

**3. Experimental Results**

We have performed five *in vivo* porcine animal tests with our Prototype II pan/tilt device. A laproscopic surgeon used this

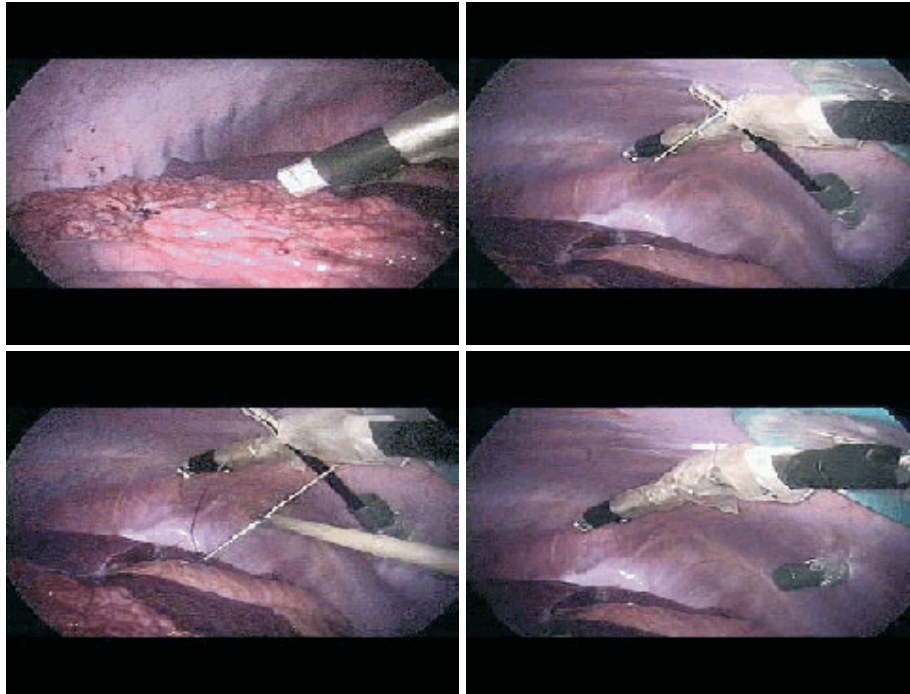


Fig. 13. Upper left: image of Prototype II camera (without zoom axis) being inserted into the abdominal cavity. Upper right: insertion of needle used to attach device to abdomen. Lower left: needle looping around device for attachment. Lower right: device firmly attached to abdominal wall.

device to perform a number of surgical procedures, including cholecystectomy (gall bladder removal), appendectomy, running (measuring) the bowel, suturing, and nephrectomy (kidney removal). Since this test animal species does not have an appendix like a human, resecting part of the colon was used to simulate an appendectomy. A short video of the experiments described below can be found at the multimedia extension (see appendix).

### 3.1. Mounting the camera

Each experiment started with the mounting of the imaging device. A porcine was under general anesthesia. A surgeon first cut small incisions into the abdominal body, then inserted trocars into the incisions. Carbon dioxide gas was pumped into the abdomen to inflate the abdominal cavity. A normal laparoscope was inserted into one trocar, and the image from the laparoscope was used to guide the mounting and orientation of our new imaging device. Figure 13 shows the mounting procedure of our imaging device onto the abdominal wall as viewed from the standard laparoscope. The surgeon inserted our device into the body through a 12 mm trocar (Figure 13, upper left). Then a needle with braided silk (SOF SILK) was inserted through the abdominal skin, which was approximately on top of the imaging device (Figure 13, upper right). Next, using

a standard laparoscopic gripper, the needle and suture were looped around the tube of imaging device, and pushed back through the abdominal wall (Figure 13, lower left). The suture was then tied off on the outside of the abdomen, securing the new device to the interior of the abdominal wall (Figure 13, lower right). The insertion trocar only contained the power and imaging wires which do not fully occupy the trocar diameter, allowing other tooling to be used through the same port. Once fixed in place, the device was used to perform the experiments described below.

Our ultimate goal is to be able to mount the camera without the assistance of a standard laparoscope, which requires an additional incision. For the experiments in this paper, we were more concerned with testing the device's functionality once it is fixed to the abdominal wall. To create true single-port surgery, we have experimented with other ways to fix the device onto the wall of the abdomen. One method, which we have implemented and used in other animal experiments, is to use an external holding mechanism. This mechanism has a rotational attachment which holds the tilt motor end of the device. When the surgeon grasps the handle of the mechanism, this attachment can rotate about  $90^\circ$ . After the device is deployed into the abdomen, the surgeon can pull the handle and rotate the device  $90^\circ$  so it is up against the abdominal wall. The disadvantage to this system is that the mechanism fills the trocar space. We have also designed, but not tested, a spring

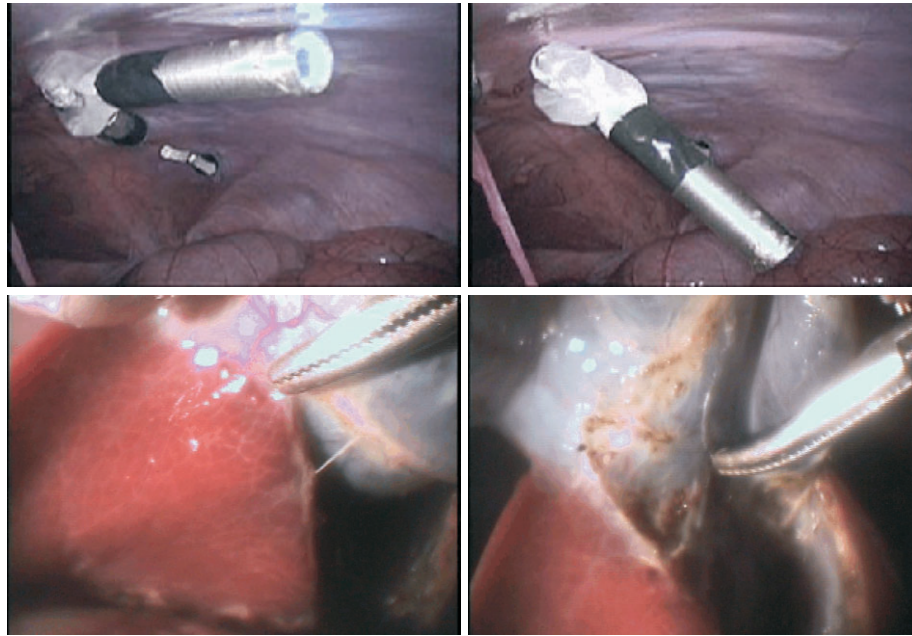


Fig. 14. Top row: Prototype II imaging device in abdominal cavity and tilt axis operating. Bottom row: images from the device during cholecystectomy.

loaded needle and suture system that can be affixed to the device and be activated to puncture the abdomen from the inside to bring the suture to the outside where it can be used to fix the device to the abdomen. A further possibility is to use magnetic anchoring (Park et al. 2007). Two internal magnetic pads can be installed in the ends of device. When the device is fully deployed into the abdomen, the surgeon can use external magnetic components to maneuver the locomotion of device outside of body. An advantage of this method is it is non-invasive, however, the intensity of the magnetic field will decrease with the increase of the abdomen's thickness, making it not suitable for all patients.

### 3.2. Experiment I

In this experiment, we used the Prototype II pan/tilt device with integrated LED light source and without zoom to perform a cholecystectomy. The upper-left and upper-right images of Figure 14 show our imaging device in the abdomen, exercising the tilt axis for viewing. These images are from a standard laparoscope. The lower-left and lower-right images of Figure 14 show the images from our device when the surgeon was performing the cholecystectomy. During the surgery, a person without laparoscopic training was operating the joystick controller by following commands from the surgeon. The surgeon's qualitative assessment of the device was *very good*. Although there was sufficient light to perform the procedures

from our device with integrated lighting, we plan to add additional lighting using more powerful LED's to enhance the images. The procedure took 21.5 minutes, which is comparable to using a standard laparoscope. Since there was only one gall bladder to remove, we were not able to perform a full comparison timing with a standard laparoscope.

### 3.3. Experiment II

In this experiment we performed a number of laparoscopic surgical procedures and compared the timings of each operation using (1) a standard laparoscope and (2) Prototype II with integrated lighting and without zoom. One of the authors (Fowler) performed the surgical procedures and personnel without laparoscopic training operated the standard laparoscope and the new devices. Figure 15 shows a series of images from the new device, which was able to pan and tilt easily to accommodate the surgeon's need for new views of the surgical site. Figure 16 shows the images of running (measuring) the bowel 150 cm using our device. During this procedure, the surgeon used a 10 cm length of umbilical tape to measure the length of bowel. By following the motion of the tools, the device can track the whole procedure. Figure 17 shows the images of a suturing procedure using the device. Finally, Figure 18 shows the images of a nephrectomy using the imaging device. The nephrectomy was a more complicated procedure that required more camera movement. The pan/tilt feature worked well to provide

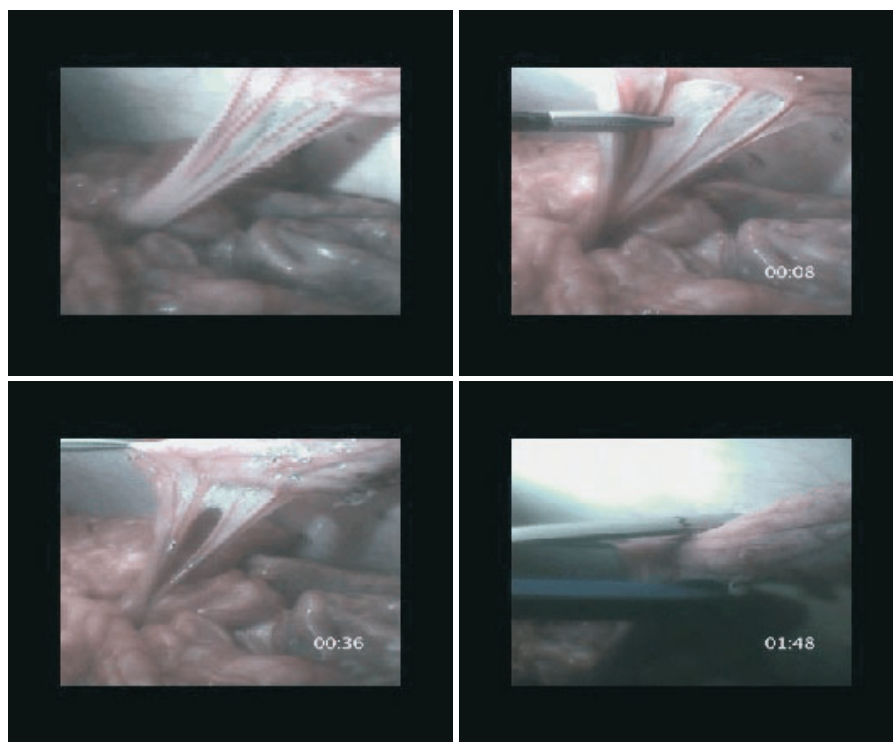


Fig. 15. Images of laparoscopic appendectomy from Prototype II.

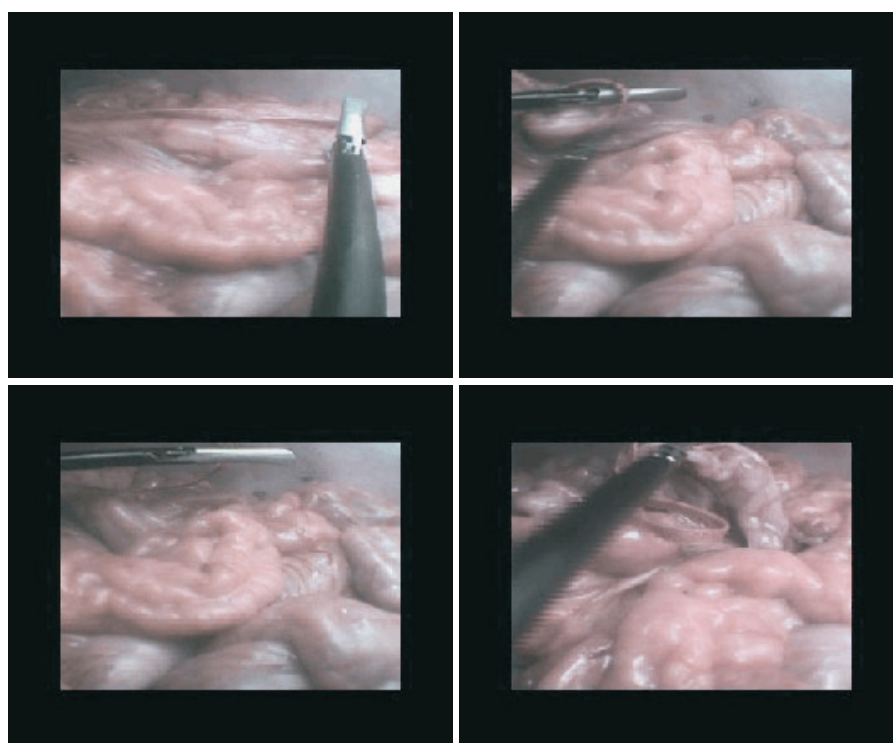


Fig. 16. Images of running the bowel from Prototype II.

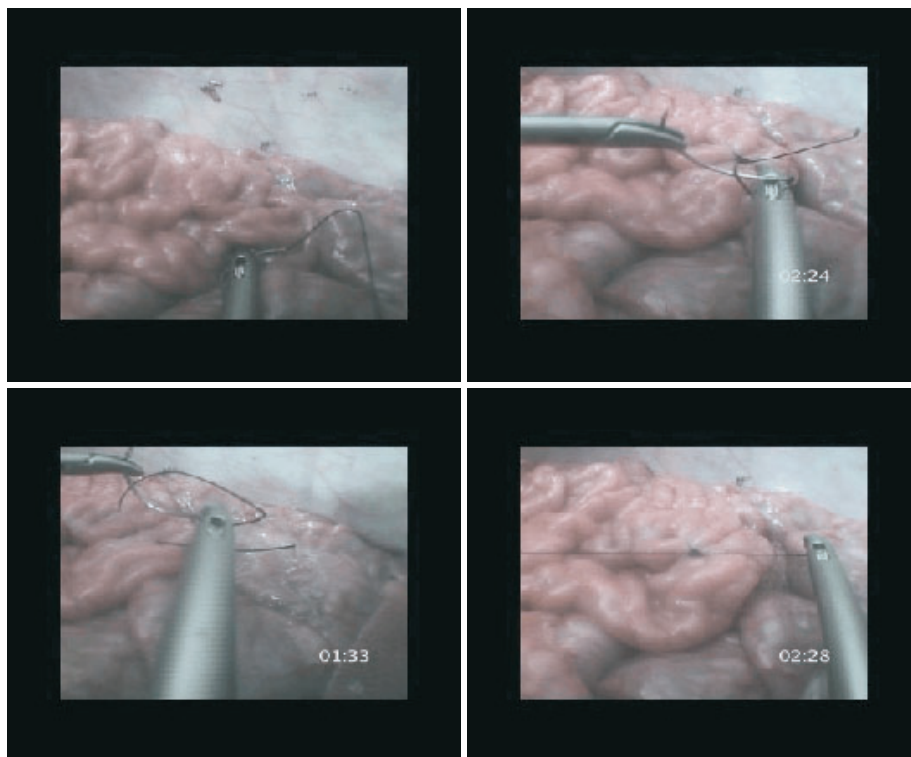


Fig. 17. Images of laparoscopic suturing from Prototype II.

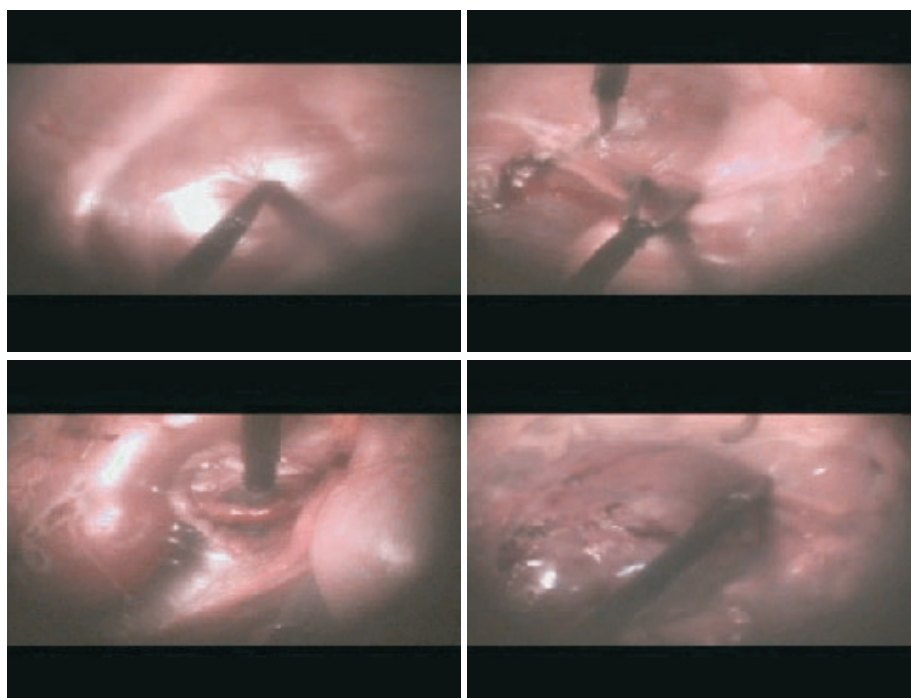


Fig. 18. Images of laparoscopic nephrectomy from Prototype II.

**Table 1. Procedure Timings**

Procedure	Device	Time (min)
Running bowel	Laparoscope	4:20
	Robot	3:30
Appendectomy	Laparoscope	2:20
	Robot	2:20
Suturing	Laparoscope	5:00
	Robot	4:00
Nephrectomy	Laparoscope	18:00
	Robot	21:00

a range of views of the site as different parts of the procedure were performed.

Table 1 shows the timing for each procedure for both a standard laparoscope and our new device. In three of the cases, using the new device did not affect the surgeon's ability to perform the procedure efficiently, and in two cases it appeared to speed up the procedure. The nephrectomy took 3 minutes longer, but was still within a timing range that was comparable to a standard laparoscope. Qualitatively, the imagery was very good, and the ease of control using intuitive commands (move left, right, up, down) with a joystick made the operational procedure simple. As this is a single experiment with a single operator, we cannot draw firm conclusions. However, it suggests that our new device may be easier to use than a normal laparoscope. We are currently running more animal experiments to further verify this hypothesis.

#### 4. Discussion and Conclusions

In this paper we have described the *in vivo* study of an imaging device for minimally invasive surgery. Our intention was to create totally insertable surgical imaging systems which do not require a dedicated surgical port, and allow more flexibility and DOFs for viewing. We performed laparoscopic cholecystectomy, appendectomy, running the bowel, suturing, and nephrectomy. The results suggest that the device may be easier to use than a normal laparoscope. There is no laparoscopic training needed for the operator of the device and by using the pan/tilt axes the device can provide a larger viewing volume than a traditional laparoscope which is restricted by the fulcrum point of insertion. We also presented a design and implementation of a pan/tilt/zoom mechanism which increases the functionality of the device.

There are tradeoffs in using our system versus a standard laparoscope. Standard laparoscopes have a rotational DOF about their long axis, allowing the image to be rotated. Our device

does not have this DOF, but we have implemented it in software image processing, which imposes an additional computational burden on the system. Our device has a diameter of 12 mm which is acceptable for most abdominal surgery, but smaller diameter (e.g. 5 mm) standard laparoscopes are commonly used, with smaller incisions and less scarring. Further research is also needed to perfect the mounting system using a single port.

We believe these insertable platforms will be an integral part of future surgical systems. The platforms can be used with tooling as well as imaging systems, allowing some surgical procedures to be performed using such a platform. The system can be extended to a multi-functional surgical robot with detachable end-effectors (grasper, cutting, dissection, and scissor). As the systems are insertable, a single surgical port can be used to introduce multiple imaging and tooling platforms into a patient.

One of our design goals was to simplify the operation and control of the imaging system. One possible approach to controlling the cameras would be to use a hybrid controller, which allows the surgeon to control some of the DOFs of the device and uses an autonomous system to control the remaining DOFs. For example, the autonomous system can control pan/tilt on the camera to keep a surgeon-identified organ in view, while the surgeon simultaneously may translate the camera to obtain a better viewing angle, all the while keeping the organ centered in the viewing field. We have developed hybrid controllers and mechanisms similar to this for robotic workcell inspection (Oh and Allen 2001) and believe we can transfer these methods for use with this device.

#### Acknowledgement

This work is supported by NIH grant 1R21EB004999-01A1.

#### Appendix: Index to Multimedia Extensions

The multimedia extension page is found at <http://www.ijrr.org>

##### Table of Multimedia Extensions

Extension	Type	Description
1	Video	<i>In vivo</i> imaging device for minimal access surgery

#### References

- Berkelman, P., Cinquin, P., Troccaz, J., Ayoubi, J., Letoublon, C. and Bouchard, F. (2002). A compact, compliant laparoscopic endoscope manipulator. *IEEE International Conference on Robotics and Automation*, pp. 1870–1875.

- Dachs, G. W., II, and Peine, W. J. (2006). A novel surgical robot design: Minimizing the operating envelope within sterile field. In *28th IEEE EMBS Annual International Conference*.
- Fuchs, G. J. (2006). Milestones in endoscope design for minimally invasive urologic surgery: the sentinel role of a pioneer. *Surgical Endoscopy*, **20**: 493–499.
- Gao, L. M., Chen, Y., Lin, L. M. and Yan, G. Z. (1998). Micro motor based new type of endoscope. *International Conference of the IEEE Engineering in Medicine and Biology Society*, Vol. 20, pp. 1822–1825.
- Geis, W. P., Kim, H. C., McAfee, P. C. and Wang, Y. (1996). Robotic arm enhancement to accommodate improved efficiency and decreased resource utilization in complex minimally invasive surgical procedures. *Proceedings of Medicine Meets Virtual Reality: Health Care in the Information Age*, pp. 471–481.
- Guthart, G. and Salisbury, K. (2000). The Intuitive telesurgery system: overview and application. *IEEE International Conference on Robotics and Automation*, pp. 618–621.
- Hu, T., Allen, P. K. and Fowler, D. L. (2007). *In vivo* pan/tilt endoscope with integrated light source. *IEEE/RSJ International Conference on Intelligent Robots and Systems (IROS)*, pp. 1284–1289.
- Hu, T., Allen, P. K., Goldman, R., Hogle, N. J. and Fowler, D. L. (2008a). *In vivo* pan/tilt endoscope with integrated light source, zoom and auto-focusing. *Stud Health Technol Inform*, **132**: 174–179.
- Hu, T., Allen, P. K., Nadkarni, T., Hogle, N. and Fowler, D. (2008b). Insertable stereoscopic 3D surgical imaging device with pan and tilt. *IEEE BioRob 2008*.
- Ikuta, K., Nokata, M. and Aritomi, S. (1994). Biomedical micro robots driven by miniature cybernetic actuator. *IEEE Workshop on Micro Electromechanical Systems*, pp. 263–268.
- Ma, J. and Berkelman, P. (2007). Task evaluation of a compact laparoscopic surgical robot system. *Proceedings of the 2007 IEEE/RSJ International Conference on Intelligent Robots and Systems*, pp. 398–403.
- Miller, A., Allen, P. and Fowler, D. (2004). *In-vivo* stereoscopic imaging system with 5 degrees-of-freedom for minimal access surgery. *Stud Health Technol Inform*, **98**: 234–240.
- Oh, P. and Allen, P. (2001). Visual servoing by partitioning degrees-of-freedom. *IEEE Transactions on Robotics and Automation*, **17**: 1–17.
- Oleynikov, D., Rentschler, M., Hadzialic, M., Dumpert, A., Platt, J. and Farritor, S. (2005). Miniature robots can assist in laparoscopic cholecystectomy. *Journal of Surgical Endoscopy*, **19**(4): 473–476.
- Park, S., Bergs, R., Eberhart, R., Baker, L., Fernandez, R. and Cadeddu, J. A. (2007). Trocar-less instrumentation for laparoscopy magnetic positioning of intra-abdominal camera and retractor. *Annals of Surgery*, **245**(3): 379–384.
- Peirs, J., Reynaerts, D., and Brussel, H. V. (2001). A miniature manipulator for integration in a self-propelling endoscope. *Sensors and Actuators*, **92**: 343–349.
- Peters, W. and Bartels, T. (1993). Minimally invasive colectomy: are the potential benefits realized? *Diseases of the Colon and Rectum*, **36**(8): 751–756.
- Schwenk, W., Bohm, B., C, C. W., Junghans, T., Grundel, K., and Muller, J. M. (1999). Pulmonary function following laparoscopic or conventional colorectal resection: a randomized controlled evaluation. *Archives of Surgery (United States)*, **134**(1): 6–12.
- Smith, W. J. (2004). *Modern Lens Design*. New York, McGraw-Hill.
- Sastry, S. S., Cohn, M. and Tendick, F. (1997). Milli-robotics for remote, minimally invasive surgery. *Robotics and Autonomous Systems*, **21**: 305–316.
- Strong, V. E. M., Hogle, N. J. and Fowler, D. L. (2005). Efficacy of novel robotic camera vs a standard laparoscopic camera. *Surgical Innovation* **12**(4): 315–318.
- Vierra, M. (1995). Minimally invasive surgery. *Annual Review of Medicine*, **46**: 147–158.
- Yu, M. (2002). M2a capsule endoscopy: a breakthrough diagnostic tool for small intestine imaging. *Gastroenterology Nursing*, **25**: 24–27.